Pharm Res (2012) 29:2902–2911
DOI 10.1007/s11095-012-0797-2

RESEARCH PAPER

Spatiotemporally Controlled Co-delivery of Anti-vasculature Agent and Cytotoxic Drug by Octreotide-Modified Stealth Liposomes

Wenbing Dai • Wu Jin • Junlin Zhang • Xueqing Wang • Jiancheng Wang • Xuan Zhang • You Wan • Qiang Zhang

Received: 15 February 2012 / Accepted: 25 May 2012 / Published online: 22 June 2012

ABSTRACT

Purpose Both combretastatin A-4 (CA-4) and doxorubicin (DOX) was loaded in different form in a targeted nanomedicine in order to achieve the active delivery of these two drugs followed by sequentially suppressing tumor vasculature and tumor cells.

Methods Octreotide-modified stealth liposomes loaded with CA-4 and DOX (Oct-L[CD]) were prepared and characterized. Then *in vitro* release, cellular uptake, *in vitro* antitumor effect, pharmacokinetics, *in vivo* sequential killing effect, *in vivo* antitumor efficacy against somatostatin receptor (SSTR) positive cells, as well as the action mechanism of such system, were studied.

Results A rapid release of CA-4 followed by a slow release of DOX was observed *in vitro*. The active targeted liposomes Oct-L[CD] showed a specific cellular uptake through ligand-receptor interaction and a higher antitumor effect *in vitro* against SSTR-positive cell line. The *in vivo* sequential killing effect of such system was found as evidenced by the fast inhibition of blood vessels and slow apoptosis-inducing of tumor cells. Oct-L[CD] also exhibited the strongest antitumor effect in MCF-7 subcutaneous xenograft models.

Conclusions Oct-modified co-delivery system may have great potential as an effective carrier for cancer therapy.

W. Dai • W. Jin • J. Zhang • X. Wang • J. Wang • X. Zhang • Q. Zhang (✉)
State Key Laboratory of Natural and Biomimetic Drugs
School of Pharmaceutical Sciences, Peking University
Beijing 100191, People's Republic of China
e-mail: zqdodo@bjmu.edu.cn

W. Dai • Y. Wan
Neuroscience Research Institute, Department of Neurobiology
School of Basic Medical Sciences, Peking University
Beijing 100191, People's Republic of China

KEY WORDS combretastatin A-4 · doxorubicin · octreotide · programmed release · spatiotemporally controlled co-delivery · targeted delivery

ABBREVIATIONS

AUC	area under the plasma concentration-time curve
CA-4	combretastatin A-4
CA-4P	combretastatin A-4 phosphate
DDS	drug delivery system
DOX	doxorubicin
DSPE-PEG (PEG Mw 2000)	1.2-distearoyl-sn-glycero-3-phosphoethanola mine-*N*-[poly(ethylene-glycol)]
DSPE-PEG-Oct	conjugate of octreotide with DSPE-PEG
EPC	egg phosphatidylcholine
FBS	fetal bovine serum
IC_{50}	50% inhibitory concentration
K	elimination rate constant
L[C]	liposomes encapsulating CA-4
L[CD]	liposomes encapsulating both CA-4 and DOX
L[D]	liposomes encapsulating DOX
Oct	octreotide
Oct-L[CD]	octreotide-targeted liposomes encapsulating both CA-4 and DOX
PBS	phosphate buffered saline
PD	pharmacodynamics
PDI	polydispersity index
PK	pharmacokinetics
SRB	sulforhodamine B
SSTR2	somatostatin receptor subtype 2

SSTRs	somatostatin receptors
$T_{1/2}$	plasma half-life
TEM	transmission electron microscope
VDAs	vascular disrupting agents
VEGF	vascular endothelial growth factor

INTRODUCTION

Although there are many encouraging progress, currently chemotherapy is far from perfect with undesirable severe side effects, low anti-tumor effect or development of drug resistance (1). Combination therapy of cancer may overcome these limitations. It could be achieved by giving two or more separate drugs, or where available, by giving a co-delivery system containing more than one active ingredient. Compared to separate drug administration, co-delivery of multiple drugs in one system has several potential advantages, including: 1) design for better synergistic effects and avoid simply use of more drugs together, 2) greatly improve the patient compliance, and 3) accurately control the individual doses and avoid the uncertainty caused by dose fractionation (2,3).

Tumor vascularization is a critical process that determines tumor growth and metastasis (4). Vascular disrupting agents are a class of novel drugs that exploit the unstable, immature characteristics of tumor blood vessels to selectively target and destroy the tumor vascular network, resulting in tumor ischemia and necrosis (5,6). Combretastatins (7), a class of small molecular tubulin-binding agents isolated from the bark of the African bush willow tree, *Combretum Caffrum*, has exhibited favorable anti-cancer activities. CA-4P, the prodrug of combretastaitin A4, has entered into clinical trials. Anti-neoplastic agents, including DOX (8) and paclitaxel (9), have been utilized in combination therapy with CA-4P against tumor in preclinical and clinic study. The anti-tumor effect of conventional chemotherapy could be greatly improved by using together with anti-vascular agents, because tumor growth and tumor metastasis are often dependent on tumor vascularization (8). Meanwhile, anti-vascular drugs induce vascular shutdown, namely a hypoxic tumor environment, which in turn activates genes that allow the cancer cell to survive and grow. So, tumor recurrence is often occurred after long term anti-vascular therapy (10). The combination therapy with both kinds of drugs can prevent the tumor recurrence and improve the anti-tumor effect. However, this combination cancer therapy failed to achieve the desired effect, likely due to: 1) tumor vascular shutdown by combretastatins prevents the accumulation of chemotherapeutic agent into tumor tissue, 2) nonspecific killing of chemotherapy still exists (11). It is supposed that spatiotemporally controlled co-delivery of both kinds of drugs may provide a new strategy for these problems.

Liposomes,with a phospholipid bilayer and a region of aqueous space inside are able to simultaneously carry the hydrophobic drug like combretastaitin A4 (CA-4) used here and hydrophilic drug DOX in the same liposomal system. It is well know that DOX can be loaded in the form of insoluble salt when prepared by the ammonium sulfate gradient remote-loading method. Therefore, the temporally controlled co-delivery of two drugs, namely, the fast release of CA-4 and slow release of DOX, could be expected.

For spatially controlled delivery, ligand-modified liposomes can increase specific interaction of liposomal drugs with targeted cells and enhance the intracellular uptake via receptor mediated endocytosis (12). Octreotide (Oct), an octapeptide analog of endogenous somatostatin, is a potential ligand due to its high affinity to somatostatin receptors (SSTRs), especially subtype 2 (SSTR2) (13), which are overexpressed in many tumors (14,15), including human small cell lung cancer cell line NCI-H446 and human breast cancer cell line MCF-7. As reported, somatostatin analogs conjugated to radioactive isotopes or cytotoxic drugs have been used for tumor diagnosis and/or treatment without any immunogenicity *in vivo*. ^{90}Y (16), ^{18}F (17), paclitaxel (18), doxorubicin (19) and camptothecin (20) have been investigated in this field, and ^{111}In-DTPA-Oct (OctreoScan®) has been approved for routine clinical scintigraphy of SSTR2-overexpressing tumors early in 1994.

With these in mind, we developed a novel Oct-modified stealth liposome system with antiangiogenic agent CA-4 in the lipid bilayer and chemotherapy agent DOX in the hydrophilic inner core. We hypothesized that the liposomes with spatial-temporal control would passively accumulate in the tumor tissue via EPR effect after intravenous injection, and rapidly release CA-4 first, cause tumor vascular shutdown and seal off the liposomal DOX into tumor tissue. And then, targeted liposomes would enter into the tumor cells via receptor mediated endocytosis and slowly release the cytotoxic drug to exert its cytotoxicity. In order to achieve the proof-of-principle for this hypotheses, after ligand density was optimized, programmed drug release *in vitro*, specific cellular uptake and antitumor effect *in vitro* in SSTR2-positive cell line were studied. Besides, the sequential effect of tumor neovasculature inhibition and tumor cell apoptosis, as well as the pharmacokinetics and antitumor efficacy *in vivo*, were also evaluated in the related animal models, respectively.

MATERIALS AND METHODS

Materials, Cells and Animals

Octreotide acetate was custom synthesized (purity 98%) by Zaichuang Biotechnology Co., Ltd. (Shanghai, China).

DSPE-PEG_{2000}-Oct was provided by State Key Laboratory of Natural and Biomimetic Drugs (Beijing, China). DSPE-PEG was purchased from NOF Co. (Tokyo, Japan). Cholesterol and Sephadex G50 were obtained from Pharmacia Biotech (Piscataway, NJ, USA), and EPC from Lipoid GmbH (Ludwigshafen, Germany). CA-4 was sourced from FWD Chemcials Co., Ltd. (Shanghai, China). Doxorubicin hydrochloride was kindly provided as a gift by Haizheng Pharmaceutical Co., Ltd. (Zhejiang, China). *In situ* cell apoptosis detection kit (TMR red) was purchased from Roche (Shanghai, China). CD31 rabbit polyclonal IgG (Abcam, UK) and SP-9000/9001/9002 immunohistochemical staining kit were from Zhongshan Golden-Bridge Biotechnology Co., Ltd. (Beijing, China). SRB was obtained from Sigma-Aldrich Inc. (Missouri, USA). All other chemicals were of analytical grade purity.

Human small cell lung cancer cell line NCI-H446, human breast cancer cell line MCF-7 were obtained from Institute of Basic Medical Sciences, Chinese Academy of Medical Sciences (Beijing, China), and cultured in RPMI 1640 medium (M&C Gene Technology, Beijing, China) supplemented with 10% FBS (Gibco, USA) at 37°C in 5% CO_2 atmosphere.

Male SD rats (180–200 g) and nude mice (18–22 g) were provided by Vital Laboratory Animal Center (Beijing, China) were acclimated at 25°C and 55% of humidity under natural light/dark conditions for 3 days before studies, with free access to standard lab food (Vital Laboratory Animal Center, Beijing, China) and water during experiments. All care and handling of animals were performed with the approval of the Institutional Animal Care and Use Committee at Peking University Health Science Center.

Preparation and Characterization of Liposomes

Liposomes encapsulating both CA-4 and DOX (L[CD]) were prepared with two steps (21,22). Firstly, lipids and drug (EPC/Cholesterol/DSPE-PEG/CA-4;25/1.28/6/2,w/w) were dissolved in chloroform in a pear-shaped flask and evaporated at 37°C on a rotary evaporator until thoroughly dry, followed by evaporation at 60°C for 30 min to enable encapsulation of CA-4 within the lipid bilayer. The resulting lipid films were hydrated with 54 mM ammonium sulfate and sonicated for 10 min at 37°C. External buffer was exchanged by eluting through a Sephadex G50 column equilibrated with PBS (pH 7.4). Then, DOX was encapsulated into above liposomes by remote loading using an ammonium sulfate gradient. Briefly, DOX was added to liposomes at a lipids-drug ratio of 20:1 (w/w) and incubated for 10 min at 60°C with gentle shaking. Free drugs were separated through a Sephadex G50 column eluted with PBS (pH 7.4). The control liposomes L[C] or L[D], only encapsulating CA-4 or DOX, respectively, was prepared in an similar procedure. The Oct-targeted liposomes (Oct-L[CD]) were prepared in accordance with the above procedure but replacing the DSPE-PEG with the mixture of DSPE-PEG-Oct and DSPE-PEG. The percentage of DSPE-PEG-Oct in total PEGylated lipids varied from 0.5% to 10% (w/w). The schematic diagram of preparation and structure of Oct-L[CD] was shown in Fig. 1.

Average particle size, PDI and Zeta Potential of liposomes were determined by dynamic light scattering using Malvern Zetasizer Nano ZS (Malvern, UK) at 25°C. Concentration of DOX was determined by UV-spectrophotometry at 485 nm, while CA-4 by HPLC-UV at 295 nm.

The morphology of Oct-L[CD] was visualized by a transmission electron microscope (TEM, JEOL, JEM-200CX, Japan) operating at an acceleration voltage of 75 kV after negative staining with uranyl acetate solution on a 200-mesh, carbon-coated copper grid.

Optimization of Octreotide Density on Liposome Surface

Approximately 5×10^5 NCI-H446 cells per well were seeded in 6-well plates 24 h prior to the study. For fine-tuning the Oct ligand density on liposomes surface, liposomes with series of Oct ligand density were added to designated wells with DOX concentration at 10 μM. After incubation for 3 h at 37°C, cells were trypsinized, washed three times with cold PBS (pH 7.4), and analyzed immediately by flow cytometry using a FACScan (BD Bioscience, CA, USA) at an excitation wavelength of 488 nm and emission wavelength of 560 nm.

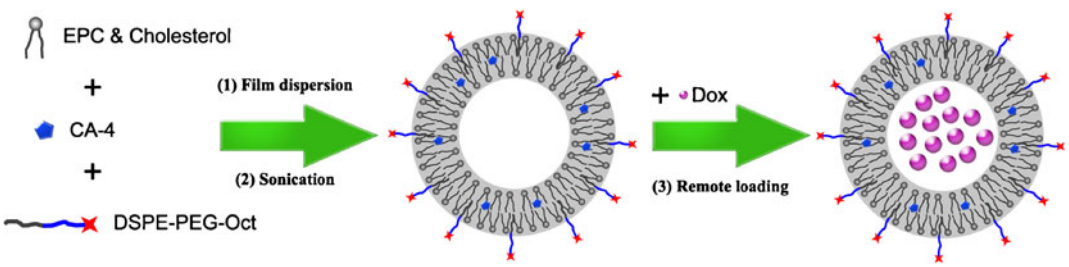

Fig. 1 Design and preparation of Oct-L[CD].

Table I Mean Diameter, Zeta Potential and Encapsulation Efficiency of Liposome Formulations (n=3)

Formulation	Size(nm)	PDI	Zeta potential (mv)	Encapsulation efficiency (%) of DOX	Encapsulation efficiency (%) of CA-4
L[C]	91.15 ± 3.42	0.27 ± 0.01	−0.88 ± 0.46	–	76.8 ± 4.8
L[D]	92.02 ± 2.68	0.22 ± 0.03	−5.27 ± 1.29	97.3 ± 2.03	–
L[CD]	97.89 ± 1.00	0.25 ± 0.03	−2.40 ± 0.78	97.0 ± 1.83	77.45 ± 2.76
Oct-L[CD]	91.43 ± 2.68	0.20 ± 0.04	−4.911 ± 1.29	97.2 ± 1.98	75.8 ± 3.15

Programmed Drug Release *In Vitro*

To determine the release kinetics of CA-4 and Dox from liposomes, 0.5 mL of liposomes were added to 0.5 mL of FBS and placed in a dialysis bag (molecular weight cut-off 3500 Da). Bags were incubated in 50 mL of PBS (pH 7.4) at 37°C with gentle shaking (100 rpm). A 0.5 mL aliquot of incubation medium were removed at predetermined time points (0.5, 1, 2, 4, 8, 12, 24, 36, 48 h) and replaced with equal volume of fresh medium. Released DOX and CA-4 were quantified by HPLC-UV method at 233 nm and 295 nm respectively.

Competition Inhibition in Cell Uptake

To investigate the mechanism of enhanced cellular uptake, NCI-H446 cells grown as monolayers in 6-well plates were pre-incubated with primary antibody (SSTR2 goat polyclonal IgG, 1:75) for 0.5 h at at 37°C to saturate receptors. Then Oct-L[CD] was added to designated wells with a final Dox concentration of 10 μM. The follow-up treatment and measurement by flow cytometry were the same as the section of "Oct Density on Liposomes Surface".

Confocal Microscopy Studies

Followed culture of NCI-H446 cells for 24 h on 14-mm^2 glass-bottom dishes, various formulations (free DOX, L[CD] or Oct-L[CD]) at a DOX concentration of 10μM were added to each dish and incubated for another 3 h at 37°C. The medium was removed and cells were washed with cold PBS followed by fixing with 4% paraformaldehyde in PBS for 10 min. Cell nuclei staining was performed with Hoechst 33258 for 10 min and the fluorescent images of cells were analyzed using laser scanning confocal microscope (LSCM, leica, TCS SP2, Germany). The exciatation/emission wavelengths of Hoechst 33258 and Dox were 352/460 nm and 480/540 nm, respectively.

In Vitro Antitumor Effect

Cytotoxicity *in vitro* was assessed in NCI-H446 cell lines. Cells were plated at the density of 5×10^3 cells per well in 200μL medium in 96-well plates and grown for 24 h, then exposed to L[CD] or Oct-L[CD] with a series of concentration for 24 h. Viability of cells was measured using SRB method. Briefly, cells were fixed with 10% trichloroacetic acid and stained, after which the excess dye was washed away by 1% acetic acid. The protein-bound dye was dissolved in 10 mM Tris base and measured at 540 nm using a 96-well plate reader (Bio-rad, 680, America) (23). The drug concentration which inhibited the cell growth by 50% was determined from semilogarithmic dose–response plots.

Sequential Killing Effect *In Vivo*

Programmed drug release *in vivo* was indirectly evaluated by immunohistochemistry on both tumor vasculature and tumor cell apoptosis. Briefly, MCF-7 tumor bearing nude mice were injected with L[CD] via the tail vein, and sacrificed at predetermined time points (1, 2, 4, 6 h). Tumors were excised on ice and immediately frozen. Thin crysections (5 μm) were made using a Reichart Cryostat, fixed in acetone and cryo-preserved. For immunohistochemistry, sections were fixed in 4% paraformaldehyde in PBS for 10 min at room temperature and blocked with 1% goat serum for 20 min. The sections were incubated

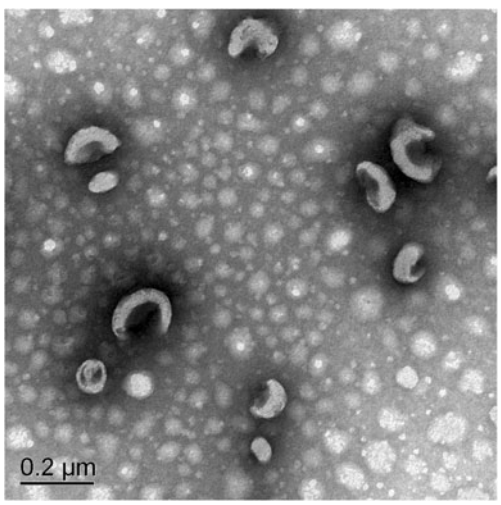

Fig. 2 TEM photomicrograph of Oct-L[CD].

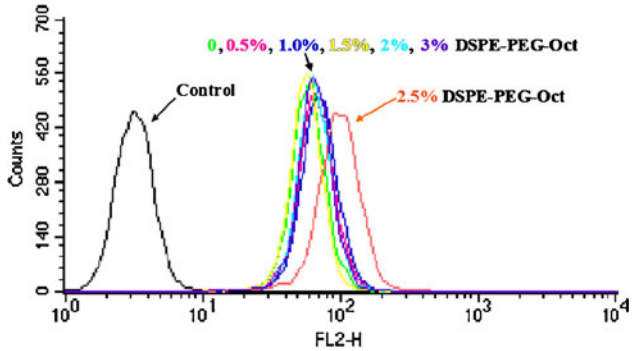

Fig. 3 Optimization of octreotide density on liposome surface by flow cytometry. NCI-H446 cells were incubated with various DOX formulations (10 μm DOX equivalent) for 3 h at 37°C.

overnight at 4°C with a primary antibody against CD31, which is an endothelial cell marker, then washed and re-incubated with a goat secondary antibody coupled with FITC for 1 h at 37°C. To further detect apoptosis signal, cryosections were processed for TUNEL staining using TMR red labeled nucleotide as the manufacturer's instructions (Roche). The sections were coated with slowfade, and imaged using laser scanning confocal microscope (LSCM, Leica, TCS SP5, Germany).

Pharmacokinetics in Rats

Male SD rats (180–200 g) were randomly divided into 3 groups (6 rats per groups) and injected intravenously through tail vein with free Dox, L[CD] or Oct-L[CD] (2.5 mg/kg for DOX and 7 mg/kg for CA-4, respectively). At predetermined time points (0.5, 1, 2, 4, 6, 8, 12, 24, 36, 48 h) after injection, whole blood samples was serially collected from retro-orbital sinus, and centrifuged for 10 min at 14000 rpm at 4°C immediately to isolate plasma and stored at −20°C. Supernatants were mixed with four-time volume of methanol to precipitate proteins, followed by centrifugation for 10 min at 14000 rpm at 4°C. The clear supernatants were detected by fluorescence spectrophotometer to determine the concentration of DOX (475 nm/580 nm) and by HPLC-UV method to determine the amount of CA-4.

Anti-tumor Activity *In Vivo*

5×10^6 MCF-7 cells per mouse were subcutaneously incubated into the right flank of nude mice to gain cancer xenografts. When tumor volume reached about 50 mm^3, mice were randomly assigned to 4 groups (n=6). Various formulations were intravenously ad ministered though the tail vein with a dose of 2 mg/kg as DOX every other day for 2 weeks. Tumor volume was measured with a vernier caliper, and calculated using the following equation:

$$\text{Volume}\left(mm^3\right) = \text{longer diameter} \times (\text{shorter diameter})^2/2$$

Tumors were also excised from sacrificed mice after 15-day's observation.

Statistical Analysis

All experiments were repeated at least three times. All data are shown as means ± SD unless particularly outlined. Student's t-test or one-way analyses of variance (ANOVA)

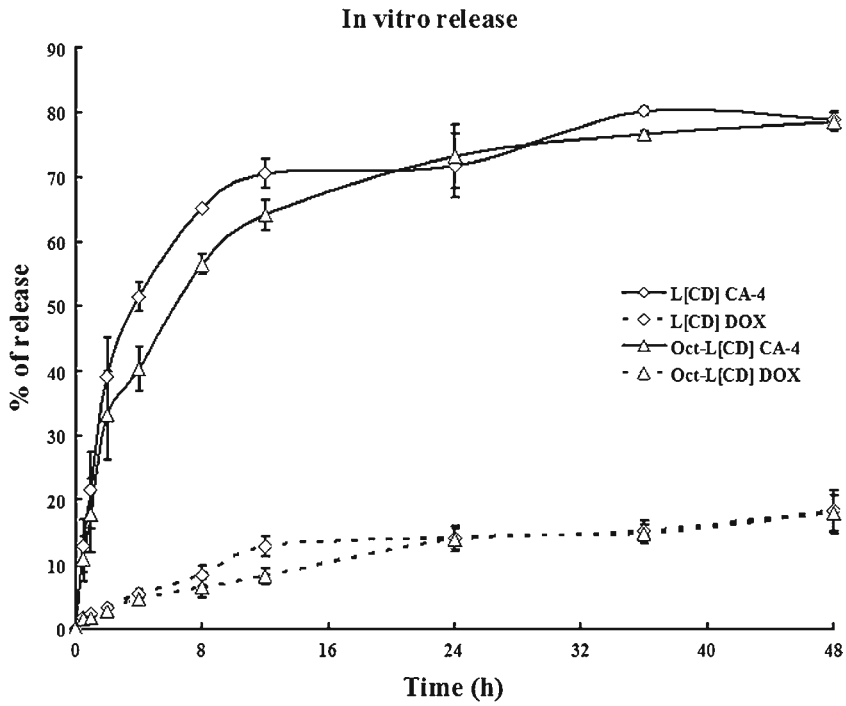

Fig. 4 Sequential release of CA-4 and DOX from L[CD] and Oct-L[CD] in FBS (50%) at 37°C.

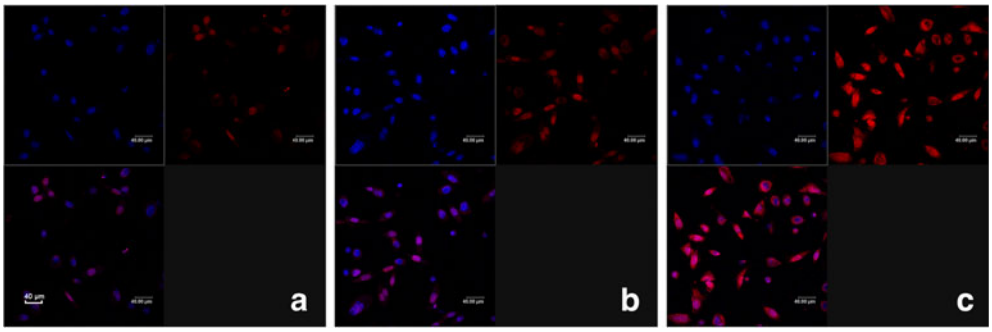

Fig. 5 Confocal Microscopy images of NCI-H446 cells treated with L[CD] (**a**), Oct-L[CD] (**b**) and free DOX group (**c**) for 3 h at 37°C. The concentration of DOX in all formulations is 10 uM. Cells were fixed with 4% formaldehyde and incubated with Hoechst 33258 for nuclei staining. Red represents fluorescence of DOX. Blue represents fluorescence of Hoechst 33258. Co-localization (lower left) of Hoechst 33258 and DOX are also presented.

were performed in statistical evaluation. A value of p less than 0.05 was considered to be significant.

RESULTS

Preparation and Characterization of Liposomes

The particle size and zeta potential of L[C], L[D], L[CD] and Oct-L[CD] are shown in Table I. As seen, all liposome formulations prepared were 90~100 nm in size (PDI<0.3) with a slight negative charge on the surface. The loading efficiency of DOX was consistently greater than 95%, while it was 70~80% for CA-4. The drug encapsulation efficiency in liposomes was not affected by Oct modification. When stored at 4°C, no significant leakage of DOX or CA-4 from liposomes was found within 2 days. The TEM image was shown in Fig. 2. The diameters determined by TEM were somewhat less than that by DLS.

Optimization of Octreotide Density on Liposome Surface

From previous studies (24–26), it was confirmed that Oct-targeted liposomes or micelles were effectively endocytosed by SSTR positive cells. Here we proceeded to optimize the Oct density on liposomes surface. We postulated that the Oct densities on the liposomes surface could be controlled by mixing quantitive DSPE-PEG-Oct with DSPE-PEG. It was indicated in Fig. 3. that the optimal Oct density was 2.5% in the test with NCI-H446 cell line. When increasing the DSPE-PEG-Oct in the formulation to 3%, there was a decrease in the cellular uptake.

Programmed Drug Release *In Vitro*

In order to simulate conditions *in vivo*, we preferred to mix liposomes with FBS directly. The profiles of drug release *versus* time *in vitro* are presented in Fig. 4. It was clear that CA-4 released from liposomes much faster than DOX. In fact, the release of CA-4 was more than 60% at 8 h, while DOX released less than 20% at 48 h, revealing a programmed release of two drugs from both liposome systems. The different release rates of two drugs were likely due to their different exsiting form in liposomes, that is, CA-4 as molecules the bilayer and DOX as insoluble salts in the inner core of liposomes (27). The release pattern between L[CD] and Oct-L[CD] was similar, suggesting little effect of Oct modification on drug release.

Selective Distribution in SSTR Positive Tumor Cells

Confocal microscopy images of NCI-H446 cells treated with different systems are given in Fig. 5. As shown in Fig. 5c, without the release process, free DOX could directly penetrate into cells through membrane diffusion, leading to the greatest extent of intracellular accumulation, which was taken as the positive control. Images of Oct-L[CD] group (Fig. 5b) displayed more red fluorescence of DOX than that of L[CD] group (Fig. 5a). This demonstrated that the surface modification with Oct

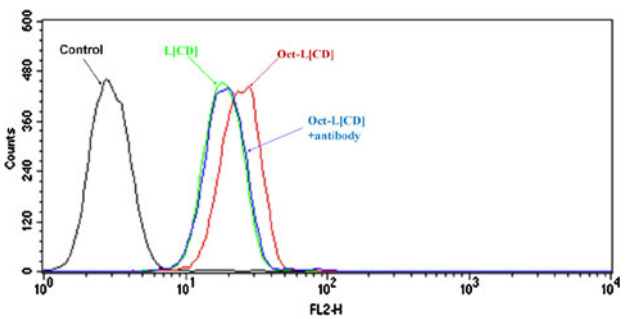

Fig. 6 Competition experiment. NCI-H446 cells were pretreated with anti-SSTR2 primary antibody at 37°C for 1 h followed by incubation with L[CD] or Oct-L[CD] for 3 h. Flow cytometric curves were obtained.

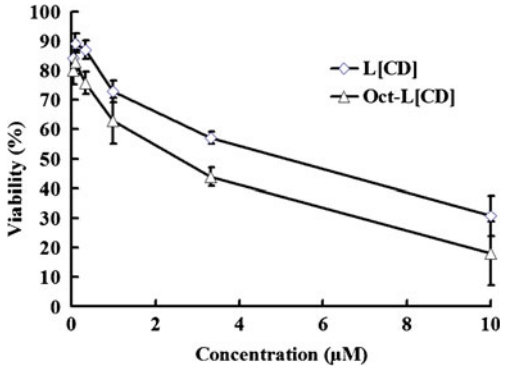

Fig. 7 Survival curves of NCI-H446 cell after exposure to L[CD] and Oct-L[CD].

could enhance the distribution of liposomal DOX into SSTR positive tumor cells.

Competition Inhibition in Cell Uptake

Competition inhibition with antibody in cellular uptake was conducted to explain the mechanism of uptake enhancement. It could be seen from Fig. 6. that Oct-L[CD] showed greater uptake by NCI-H446 cells than L[CD]. However, when the cells were pretreated with primary antibody (anti-SSTR2), the uptake of Oct-L[CD] was significantly inhibited, which was very close to that of L[CD]. In other words, the increase of cell uptake in Oct-L[CD] group was indeed attributed to the interaction between Oct and its receptor SSTR2.

Antitumor Effect *In Vitro*

The IC_{50} values of liposomal DOX were determined from dose-dependent cell inhibition curves obtained in a SRB assay. As shown in Fig. 7, the IC_{50} values against NCI-H446 cell lines for L[CD] and Oct-L[CD] groups were $1.47 \pm 0.12 \mu M$ and $5.17 \pm 0.41 \mu M$, respectively. As expected, the antitumor effect of Oct-L[CD] was stronger than that of L[CD] ($p < 0.05$), and this may be related to the enhanced cell uptake in Oct-L[CD] group.

Sequential Killing Effect *In Vivo*

In order to verify whether the liposomal system take effects sequentially *in vivo*, tumor apoptosis by DOX was detected by TUNEL (TdT-mediated Dutp nick end labeling) and neovasculature inhibition by CA-4 was evaluated simultaneously by immunostaining with anti-CD31. As shown in Fig. 8a, the L[CD] induced significant inhibition on the tumor vasculature at the beginning, evidenced by the presence of obvious green fluorescence of FITC labeling CD31. And the green fluorescence almost disappeared after 2 h. On the other hand, significant tumor cell apoptosis appeared until 4 h after administration and became even stronger after 6 h (Fig. 8b). In general, the sequential killing effect of these two drugs *in vivo* was proved, which was consistent with the sequential drug release *in vitro*.

Pharmacokinetics Study in Rats

The plasma drug concentrations *versus* time are illustrated in Fig. 9. The main pharmacokinetic parameters related are shown in Tables II and III, respectively. It was found that the elimination of free DOX was rather fast since it was only detectable at 0.5 h, the concentration of which is about 0.024 μg/mL. With a similar AUC value, the two liposomal DOX groups prolonged the drug levels significantly as shown in Fig. 9. Oct-L[CD] group showed a faster elimination of DOX than L[CD] group (Table II), indicating that the long-circulation effect of PEGylated liposomes was

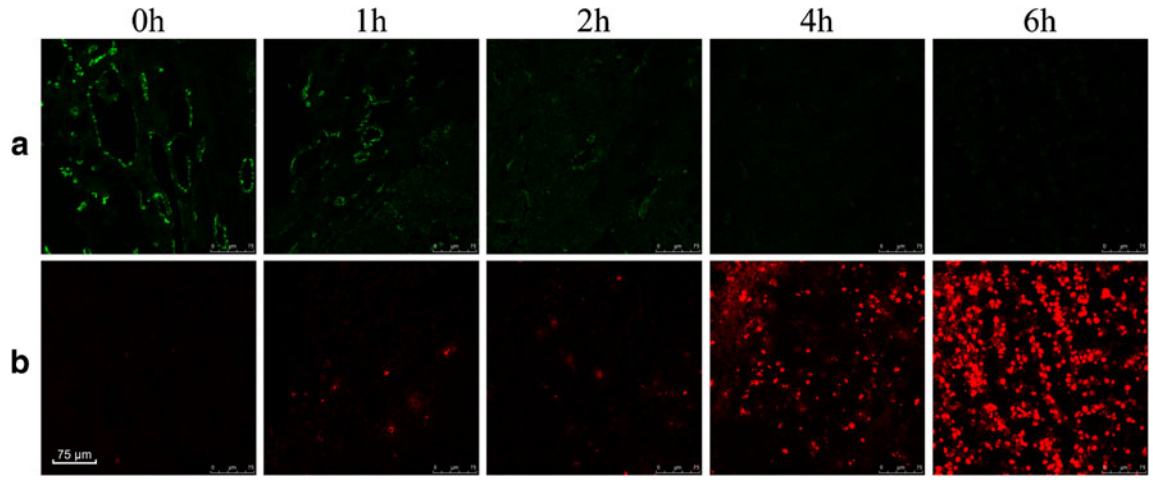

Fig. 8 Programmed suppression effect of L[CD] on tumor vasculature and apoptosis. (**a**) Vasculature staining with anti-CD31 antibody labeled by FITC at different time points after administration. (**b**) Tumor TUNEL-labeled for apoptosis with the use of TMR red-labeled nucleotide.

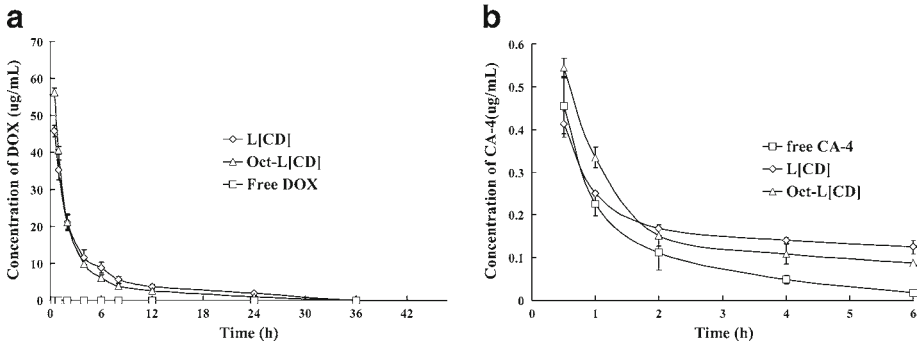

Fig. 9 Pharmacokinetics of doxorubicin (**a**) and CA-4 (**b**) encapsulated in liposomes in SD mice.

affected but partially maintained after the Oct modification. Again, Oct-L[CD] group exhibited a faster elimination of CA-4 than L[CD] group (Fig. 9b).

Anti-tumor Effect *In Vivo*

The anticancer efficacy of different formulations is displayed in Fig. 10. As seen Fig. 10a, the tumor volume was always the smallest at each test point in Oct-L[CD] group, suggesting its stronger inhibition effect on solid tumor than other groups ($p < 0.05$). The excised tumors in Oct-L[CD] group were also the smallest at the end of the test (Fig. 10b). The results were in accordance with the antitumor study and cell uptake *in vitro*.

DISCUSSION

Oct-L[CD] and L[CD] were investigated *in vitro* and *in vivo* in this study, in order to prove the hypothesis that spatio-temporally controlled co-delivery of both anti-vasculature agent and cytotoxic drug by Oct-modified liposomes may enhance the therapeutic effects.

Sengupta S *et al.* firstly reported the co-delivery of combretastatin and doxorubicin (22), but our system is different mainly in two aspects: the active targeting by Oct modification and the simple physical encapsulation of both drugs in stealth liposomes. In fact, we combine the active delivery by Oct conjugation and the combination therapy of these two drugs with sequential release in this study, which is also different from our previous reports (21,25).

As can be seen from Table I, the mean diameter, zeta potential and encapsulation efficiency of Oct-L[CD] were generally similar to those of L[CD], which demonstrated that the modification with Oct had little effects on physicochemical properties of liposomes. CA-4 is a lipophilic drug and only can be incorporated into the lipid bilayer membrane, while DOX can be loaded into the hydrophilic core in the form of insoluble salt by the ammonium sulfate gradient remote-loading method. So it was easy to understand that the encapsulation effiency of CA-4 was lower than that of DOX.

The programmed drug release of CA-4 and DOX was demonstrated *in vitro* and also validated *in vivo* by immunohistochemistry on both tumor vasculature inhibition and tumor cell apoptosis in this study. The sequential release of CA-4 and DOX resulted in temporal effect on respective target. As shown in Fig. 7, there was a rapid collapse of the vasculature because of the first and rapid release of CA-4 and then the tumor cells began to apoptosis as the gradually release of DOX. Owing to the similar drug release behaviors between Oct-L[CD] and L[CD], we have only studied the sequential killing effect of L[CD] to validate the concept of temporally control of co-delivery systems. The good correlation between the programmed release profile *in vitro* and their sequential effect *in vivo* indicated the possibility of improved tumor therapy by temporally controlled drug delivery.

On the other hand, more exactly controlled release of doxorubicin and combretastatin is also needed. For the given drugs and given liposome system as mentioned above, the drug release rates may depend on the lipid components, the ratio of lipids, drug concentration and so on. For instance, the EPC/cholesterol ratio may impact the flowability of lipid membrane and different drug loading may result in different concentration gradient, leading to different release rate for each drug, which needs further investigations.

Table II Main Pharmacokinetic Parameters of DOX in Plasma After Intravenous Administration of L[CD] or Oct-L[CD] to Rats ($n=6$)

Formulation	AUC((μg/mL)·h)	k(1/h)	$t_{1/2}$(h)
L[CD]	143.18 ± 32.3	0.38 ± 0.10	1.89 ± 0.42
Oct-L[CD]	131.75 ± 15.7	0.56 ± 0.10**	1.26 ± 0.20*

** $P < 0.01$: *vs* L[CD] * $P < 0.05$: *vs* L[CD]

Table III Main Pharmacokinetic Parameters of CA-4 in Plasma After Intravenous Administration of Free CA-4, L[CD] or Oct-L[CD] to Rats ($n=6$)

Formulation	AUC((μg/mL)·h)	k(1/h)	$t_{1/2}$(h)
Free CA-4	0.54 ± 0.14	1.10 ± 0.48	0.73 ± 0.34
L[CD]	0.81 ± 0.04	0.26 ± 0.07*	2.73 ± 0.66*
Oct-L[CD]	0.74 ± 0.04	0.80 ± 0.37*#	1.01 ± 0.51*#

* $P < 0.05$: *vs* free CA-4, # $P < 0.05$: *vs* L[CD]

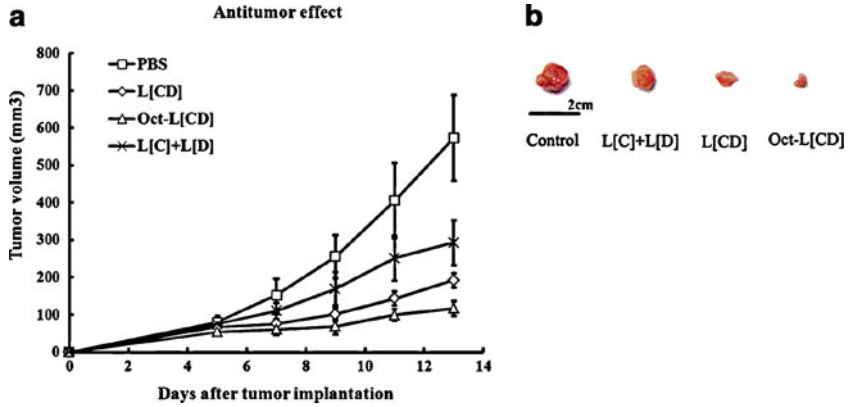

Fig. 10 Antitumor efficiency of different treatments in MCF-7-bearing subcutaneous tumor models in nude mice. (**a**) Tumor volumes *versus* time. Data represent mean ± SD (n=6). (**b**) Tumors excised at the end of the tests.

Ligand-targeted liposomes have been investigated intensely in an effort to further enhance the selectivity and effectiveness of liposomal drug by receptor-ligand interaction and subsequent endocytosis. Moreover, the ligand density on liposomes surface has an effect on intracellular uptake of the liposomes. SSTRs, the receptors of Oct, have been proved to be highly expressed on the surface of mult-type tumor cells. In this study, we choose NCI-H446 and MCF-7 because they are proved to be the SSTR2-positive cell lines (24).

As demonstrated in Fig. 3, a proper Oct density on the surface of liposomes is favorable for the cellular uptake, namely, under or over modification is not recommended. This may be related to both the receptor density on the cell surface and the steric hindrance at the binding site between the receptor and ligand (28,29). In addition, the excess modification would mask the antibiofouling properties of PEG which is relevant to the long circulation of lipsomes *in vivo*. Some similar finding has been reported previously (25,30).

As seen in Fig. 4, the DOX release was very slow for both liposomal systems, much less than 5% within 3 h, and the cell uptake was recorded after 3 h incubation (Fig. 5), so the extracellular release of DOX in the process of incubation might have little effect on the observation of cell uptake in Fig. 5. The results of cellular uptake studies and the following competition inhibition studies demonstrated that the enhanced intracellular uptake of Oct-L[CD] by NCI-H446 cells was mediated by a mechanism of ligand-receptor interaction, especially the Oct-SSTR2 interaction. The results of *in vitro* antitumor test also agreed with the cellular uptake studies, namely, the enhanced internalization of liposomal DOX by Oct-modification resulted in an increasing antitumor efficacy. These observations were also in good accord with the enhanced uptake on other cell lines in previous studies (25,26).

It was clear from Fig. 9 and Tables II and III, that liposomal formulations could significantly prolonged the concentration of two drug loaded, and the elimination of drug in Oct-L[CD] group was faster than the non-modified liposomes. A number of studies have demonstrated the faster clearance of ligand targeted liposomes (31–33). Furthermore, the doses by intravenous injection were 2.5 mg/kg for DOX and 7 mg/kg for CA-4, respectively. In Fig. 9a and b, the plasma concentration of CA-4 was much lower than that of DOX in the experimental period. This may be partly owing to the rapid release of CA-4 in comparison with that of DOX. In other words, *in vivo* pharmacokinetic test further confirmed the programmed release feature of the two drugs from L[CD].

Results in Fig. 10 indicated that treatment with L[CD] produced a significant inhibition of tumor growth compared to the co-administration of L[C] and L[D], which might attribute to the temporally controlled release of CA-4 and DOX in L[CD] system. CA-4 was described as a strong cell growth and tubulin inhibitor that induced the disruption of vascular function, causing the selective and irreversible damage to the neovasculature of tumors. Here, CA-4 in the outer bilayer released first, causing vascular shutdown and cutting off the supply of nutrients and oxygen. Then DOX in the inner core play its role in killing tumor cells. The strongest antitumor effect of Oct-L[CD] might be an integrated result of ligand-targeting and programmed release of drugs with different targets. By the way, the free DOX was not used as the control in our efficacy study, because of its fast elimination and low concentration as shown in pharmacokinetic study (Fig. 9). Besides, the advantage of liposomal DOX over free DOX was demonstrated in many reports (34–36).

CONCLUSIONS

Herein we have successfully constructed a novel liposomal delivery system through the surface modification with Oct and temporal delivery of traditional chemotherapy drug doxorubicin and anti-angiogenesis agent combretastatin A4. This system showed programmed drug release *in vitro* and also the sequential killing effects of these two drugs *in vivo*. The Oct-targeted co-delivery liposomes also exhibited the best anti-tumor effect on nude mice bearing MCF-7 tumors. It is concluded that the liposome system based on spatiotemporal design may be a potential drug delivery system for the treatment of malignant solid tumors.

ACKNOWLEDGMENTS AND DISCLOSURES

This study was supported by the National Nature Science Foundation (No.81130059), National Basic Research Program of China (No. 2009CB930300).

REFERENCES

1. Lisa BP, James OB. Nanoparticle and targeted systems for cancer therapy. Adv Drug Deliv Rev. 2004;56:1649–59.
2. Zhang L, Radovic-Moreno AF, Alexis F, Gu FX, Basto PA, Bagalkot V, Jon S, Langer RS, Farokhzad OC. Co-delivery of hydrophobic and hydrophilic drugs from nanoparticle-aptamer bioconjugates. Chem Med Chem. 2007;2:1268–71.
3. Mitragotris S. Synergistic effect of enhancers for transdermal drug delivery. Pharm Res. 2000;17:1354–59.
4. Folkman J. Role of angiogenesis in tumor growth and metastasis. Semin Oncol. 2002;29:15–8.
5. Siemann DW, Chaplin DJ, Horsman MR. Vascular-targeting therapies for treatment of malignant disease. Cancer. 2004;100:2491–97.
6. Thorpe PE. Vascular targeting agents as cancer therapeutics. Clin Cancer Res. 2004;10:415–27.
7. Dziba JM, Marcinek R, Venkataraman G, Robinson JA, Ain KB. Combretastatin A4 phosphate has primary antineoplastic activity against human anaplastic thyroid carcinoma cell lines and xenograft tumors. Thyroid. 2002;12:1063–70.
8. Nelkin BD, Ball DW. Combretastatin A-4 and doxorubicin combination treatment is effective in a preclinical model of human medullary thyroid carcinoma. Oncol Rep. 2001;8:157–60.
9. Yeung SC, She M, Yang H, Pan J, Sun L, Chaplin D. Combination chemotherapy including combretastatin A4 phosphate and paclitaxel is effective against anaplastic thyroid cancer in a nude mouse xenograft model. J Clin Endocrinol Metab. 2007;92:2902–09.
10. Verheul HMW, Voest EE, Schlingemann RO. Are tumours angiogenesis-depent? J Pathol. 2004;202:5–13.
11. Lee SM, Woll PJ, Rudd R, Ferry D, O'Brien M, Middleton G, Spiro S, James L, Ali K, Jitlal M, Hackshaw A. Anti-angiogenic therapy using thalidomide combined with chemotherapy in small cell lung cancer: a randomized, double-blind, placebo-controlled trial. J Natl Cancer Inst. 2009;101:1049–57.
12. Sapra P, Tyagi P, Allen TM. Ligand-targeted liposomes for cancer treatment. Curr Drug Deliv. 2005;2:368–81.
13. Bauer W, Briner U, Doepfner W, Haller R, Huguenin R, Marbach P, Petcher TJ, Pless J. SMS 201-995: a very potent and selective octapeptide analogue of somatostatin with prolonged action. Life Sci. 1982;31:1133–40.
14. Reubi JC, Kvols L, Krenning E, Lamberts SW. Distribution of somatotatin receptors in normal and tumor tissue. Metabolism. 1990;39:78–81.
15. Volante M, Rosas R, Allia E, Granata R, Baragli A, Muccioli G, Papotti M. Somatostatin, cortistatin and their receptors in tumours. Mol Cell Endocrinol. 2008;286:219–29.
16. Wild D, Schmitt JS, Ginj M, Mäcke HR, Bernard BF, Krenning E, De Jong M, Wenger S, Reubi JC. DOTA-NOC, a high-affinity ligand of somatostatin receptor subtypes 2, 3 and 5 for labelling with various radiometals. Eur J Nucl Med Mol Imaging. 2003;30:1338–47.
17. Ginj M, Schmitt JS, Chen J, Waser B, Reubi JC, de Jong M, Schulz S, Maecke HR. Design, synthesis, and biological evaluation of somatostatin-based radiopeptides. Chem Biol. 2006;13:1081–90.
18. Shen H, Hu D, Du J, Wang X, Liu Y, Wang Y, Wei JM, Ma D, Wang P, Li L. Paclitaxel–octreotide conjugates in tumor growth inhibition of A549 human non-small cell lung cancer xenografted into nude mice. Eur J Pharmacol. 2008;601:23–9.
19. Lasfer M, Vadrot N, Schally AV, Nagy A, Halmos G, Pessayre D, Feldmann G, Reyl-Desmars FJ. Potent induction of apoptosis in human hepatoma cell lines by targeted cytotoxic somatostatin analogue AN-238. J Hepatol. 2005;42:230–37.
20. Moody TW, Fuselier J, Coy DH, Mantey S, Pradhan T, Nakagawa T, Jensen RT. Camptothecin-somatostatin conjugates inhibit the growth of small cell lung cancer cells. Peptides. 2005;26:1560–66.
21. Zhang YF, Wang JC, Bian DY, Zhang X, Zhang Q. Targeted delivery of RGD-modified liposomes encapsulating both combretastatin A-4 and doxorubicin for tumor therapy: *In vitro* and *in vivo* studies. Eur J Pharm Biopharm. 2010;74:467–73.
22. Sengupta S, Eavarone D, Capila I, Zhao G, Watson N, Kiziltepe T, Sasisekharan R. Temporal targeting of tumour cells and neovasculature with a nanoscale delivery system. Nature. 2005;436:568–72.
23. Vichai V, Kirtikara K. Sulforhodamine B colorimetric assay for cytotoxicity screening. Nat Protoc. 2006;1:1112–16.
24. Zhang J, Jin W, Wang X, Wang J, Zhang X, Zhang Q. A novel octreotide modified lipid vesicle improved the anticancer efficacy of doxorubicin in somatostatin receptor 2 positive tumor models. Mol Pharm. 2010;7:1159–68.
25. Zhang Y, Wang X, Wang J, Zhang X, Zhang Q. Octreotide-modified polymeric micelles as potential carriers for targeted docetaxel delivery to somatostatin receptor overexpressing tumor cells. Pharm Res. 2011;28:1167–78.
26. Sun M, Wang Y, Shen J, Xiao Y, Su Z, Ping Q. Octreotide-modification enhances the delivery and targeting of doxorubicin-loaded liposomes to somatostatin receptors expressing tumor *in vitro* and *in vivo*. Nanotechnology. 2010;21:475101–12.
27. Fritze A, Hens F, Kimpfler A, Schubert R, Peschka-Süss R. Remote loading of doxorubicin into nanoliposomes driven by a transmembrane phosphate gradient. Biochim Biophys Acta. 2006;1758:1633–40.
28. Gu F, Zhang L, Teply BA, Mann N, Wang A, Radovic-Moreno AF, Langer R, Farokhzad OC. Precise engineering of targeted nanoparticles by using self-assembled biointegrated block copolymers. Proc Natl Acad Sci USA. 2008;105:2586–91.
29. Cairo CW, Gestwicki JE, Kanai M, Kiessling LL. Control of multivalent interactions by binding epitope density. J Am Chem Soc. 2002;124:1615–19.
30. Jule E, Nagasaki Y, Kataoka K. Lactose-installed poly(ethylene glycol)-poly(d, l-lactide) block copolymer micelles exhibit fast-rate binding and high affinity toward a protein bed simulating a cell surface. A surface plasmon resonance study. Bioconjug Chem. 2003;14:177–86.
31. Emanuel N, Kedar E, Bolotin E, Smorodinsky NI, Barenholz Y. Targeted delivery of doxorubicin via sterically stabilized immunoliposomes: pharmacokinetics and biodistribution in tumor-bearing mice. Pharm Res. 1996;13:861–68.
32. Turka MJ, Watersb DJ, Low PS. Folate-conjugated liposomes preferentially target macrophages associated with ovarian carcinoma. Cancer Lett. 2004;213:165–72.
33. Linuma H, Maruyama K, Okinaga K. Intracellular targeting therapy of cisplatin-encapsulated transferrin-polyethylene glycol liposomes on peritoneal dissemination of gastric cancer. Int J Cancer. 2002;299:130–37.
34. Mayer LD, Bally MB, Cullis PR, Wilson SL, Emerman JT. Comparison of free and liposome encapsulated doxorubicin tumor drug uptake and antitumor efficacy in the SC115 murine. Cancer Lett. 1990;53(2–3):183–90.
35. Lu WL, Qi XR, Zhang Q, Li RY, Wang GL, Zhang RJ, Wei SL. A pegylated liposomal platform: pharmacokinetics, pharmacodynamics, and toxicity in mice using doxorubicin as a model drug. J Pharmacol Sci. 2004;95(3):381–9.
36. Gabizon AA. Pegylated liposomal doxorubicin: metamorphosis of an old drug into a new form of chemotherapy. Cancer Invest. 2001;19(4):424–36.